

[Click here to view linked References](#)

A new pachypleurosaur (Reptilia: Sauropterygia) from the Middle Triassic of southwestern China and its phylogenetic and biogeographic implications

Yi-Wei Hu¹, Qiang Li^{1,2}, Jun Liu^{1*}

¹ School of Resources and Environmental Engineering, Hefei University of Technology, Hefei 230009, China. ² Institute of Geosciences, University of Bonn, Bonn 53115, Germany

*Correspondence: junliu@hfut.edu.cn

Abstract

After the devastating Permo-Triassic Mass Extinction, several new groups of large reptilian predators invaded the sea in the early part of the Triassic. Among these predators, sauropterygians, consisting of placodonts, pachypleurosaurs, nothosaurs and pistosaurs (including the iconic plesiosaurs), displayed the greatest diversity at both the generic and species levels, and persisted from the Early Triassic to the Late Cretaceous. Here we report a new species of Pachypleurosauria, *Dianmeisaurus mutaensis* sp. nov., from a recently discovered Lagerstätte in the Upper Member of the Anisian Guanling Formation. The only known specimen of the new species was collected from a quarry near Muta village, Luxi County, Yunnan Province, South China. Our new phylogenetic analysis based on a novel data matrix recovered the new taxon as a sister group to *Dianmeisaurus gracilis* – a small pachypleurosaur from the Middle Triassic Luoping biota. The new phylogenetic analysis also collapsed the

monophyly of the traditionally recognized Eusauropterygia. Pistosauroidea, *Majiashanosaurus*, and *Hanosaurus* comprise the consecutive sister groups to a new clade including Pachypleurosauria and Nothosauroidea. A monophyletic Pachypleurosauria, within which the clade consisting of *Dianmeisaurus* and *Panzhousaurus* occupies the basal-most position, is recovered by this study. The clade consisting of *Dawazisaurus* and *Dianopachysaurus* forms the sister group to the remaining pachypleurosaurs included in this study. Since *Dianmeisaurus*, *Panzhousaurus*, *Dawazisaurus*, and *Dianopachysaurus* are all exclusively known from South China, our study provides further evidence to the hypothesis that pachypleurosaurs had a palaeobiogeographic origin in the eastern Tethys.

Keywords: marine reptiles, Pachypleurosauria, *Dianmeisaurus*, phylogeny, palaeobiogeographic origin

Introduction

The Sauropterygia is the most flourishing clade among Mesozoic marine reptiles in terms of species diversity, and includes the iconic Plesiosauroidea from the Jurassic and Cretaceous and the stem-group Placodontia and Eosauropterygia from the Triassic (Kelley et al., 2014; Li & Liu, 2020; Motani, 2009; Rieppel, 2000; Stubbs & Benton, 2016). Eosauropterygians were traditionally divided into three groups, the Pachypleurosauria, the Nothosauroidea, and the Pistosauroidea (Rieppel, 2000). This traditional view holds that a monophyletic Pachypleurosauria comprises the sister

group to the clade Eusauropterygia consisting of Nothosauroida and Pistosauroida (Lin et al., 2021; Liu et al., 2011; Neenan et al., 2013; Rieppel, 2000).

Since the review by Rieppel (2000), many new genera of basal eosauropterygians have been described from the Triassic of China and Europe (Cheng et al., 2006; Cheng et al., 2012; Cheng et al., 2016; Dalla Vecchia, 2006; de Miguel Chaves et al., 2018; Jiang et al., 2019; Jiang et al., 2008; Klein et al., 2022; Liu et al., 2011; Ma et al., 2015; Marquez-Aliaga et al., 2019; Renesto et al., 2014; Shang et al., 2020; Shang & Li, 2015; Shang et al., 2011; Xu et al., 2022; Xu et al., 2023), which has complicated eosauropterygian interrelationships. Holmes et al. (2008) restudied *Keichousaurus hui* and questioned the monophyly of Pachypleurosauria for the first time, which has been supported by several later studies (e.g., Cheng et al., 2012; Cheng et al., 2016; Jiang et al., 2014; Marquez-Aliaga et al., 2019; Shang et al., 2011; Shang & Li, 2015; Shang et al., 2017; Wu et al., 2011). Their results also showed the collapse of a monophyletic Eusauropterygia clade, which was supported by some independent studies (e.g., Li & Liu, 2020; Liu et al., 2021; Neenan et al., 2013; Xu et al., 2022, 2023), although these studies recognized a monophyletic Pachypleurosauria. The study by Ma et al. (2015) supported the collapse of a monophyletic Pachypleurosauria, but still recognized a monophyletic Eusauropterygia clade instead. This finding was also supported by some other studies (e.g., Liu et al., 2015; Shang et al., 2020; Jiang et al., 2019).

1 61 Although the above-mentioned new Triassic basal eosauropterygian taxa have been
2
3
4 62 well described, the phylogenetic analysis associated with the description of these new
5
6 63 taxa primarily relied on slightly expanded data matrices that originated from Rieppel
7
8
9 64 et al. (2002). Thus, the morphological information provided by comparative studies of
10
11
12 65 these new materials of basal eosauropterygians still needs to be incorporated to
13
14
15 66 examine the phylogenetic interrelationships of eosauropterygians. Additionally, the
16
17
18 67 palaeobiogeographic origin of Pachypleurosauria is still controversial (Klein et al.,
19
20
21 68 2022; Liu et al., 2011; Renesto et al., 2014; Rieppel, 1999a; Rieppel & Lin, 1995; Xu
22
23
24 69 et al., 2023). Pachypleurosaurs have been reported in both the western Tethys (the
25
26
27 70 Germanic Basin, Alpine Triassic, and Iberian Peninsula) (e.g., Čerňanský et al., 2018;
28
29
30 71 de Miguel Chaves et al., 2020; Klein et al., 2022; Renesto et al., 2014; Rieppel, 1989;
31
32
33 72 Sander, 1989; Sues & Carroll, 1985) and the eastern Tethys (South China and
34
35
36 73 Myanmar) (e.g., Liu et al., 2011; San et al., 2019; Shang & Li, 2015; Jiang et al.,
37
38
39 74 2019). Rieppel and Lin (1995) proposed an eastern Tethys origin of pachypleurosaurs
40
41
42 75 based on the phylogenetic result that shows *Keichousaurus* from China forms the
43
44
45 76 sister group of all European pachypleurosaurs. This hypothesis was supported by Liu
46
47
48 77 et al. (2011) and Renesto et al. (2014). However, the earliest known pachypleurosaurs
49
50
51 78 is *Dactylosaurus* from the early Anisian of the Germanic Basin (Rieppel & Hagdorn,
52
53
54 79 1997). Thus, the palaeobiogeographic origin of pachypleurosaurs is more complex
55
56
57 80 than previously believed and needs to be reassessed (Klein et al., 2022).
58
59
60
61
62
63
64
65

1 81 In this paper, we report a new species of Pachypleurosauria from Yunnan Province,
2
3
4 82 China, represented by the part and counterpart of a single individual. The new
5
6 83 specimen shares several synapomorphies with *Dianmeisaurus gracilis*, but also
7
8
9 84 presents several unique characteristics meriting the status of a new species. In
10
11
12 85 addition to describing the new species in detail, we also aim to clarify the
13
14
15 86 phylogenetic interrelationships of eosauropterygians by incorporating the
16
17
18 87 morphological information from the recently described basal eosauropterygian taxa
19
20
21 88 and discuss the palaeobiogeographic origin of pachypleurosaurs.
22
23
24

25 89 **Materials and methods**

26
27 90 The new specimen described here was collected from the Upper Member of the
28
29
30 91 Anisian Guanling Formation in an abandoned quarry that is about one km northwest
31
32
33 92 of Muta village, Luxi County, Yunnan Province (Fig. 1). The skeleton was split into
34
35
36 93 two parts during collection and prepared with pneumatic tools and needles in the
37
38
39 94 palaeontological lab of HFUT. The data matrix for the phylogenetic analysis was
40
41
42 95 produced using the software Mesquite Version 3.6. The data matrix comprises 203
43
44
45 96 characters, of which 179 are from Li and Liu (2020), 17 from Lin et al. (2021), three
46
47
48 97 from Klein et al. (2022), and four are new characters. Published character codings
49
50
51 98 were carefully checked, and several errors were corrected (the character list and data
52
53
54 99 matrix are given in Supplementary Data 1 and 2, respectively). Cladistic analysis was
55
56
57 100 performed using the software PAUP Version 4.0a169 for Windows (Swofford, 2021).
58
59
60
61
62
63
64
65

Heuristic search (ADDSEQ = RANDOM, NREPS = 1000, HOLD = 100, with other settings default) was performed to acquire the most parsimonious trees. Bootstrap support values were estimated by 1000 replicates and other settings were default. Measurements were collected using digital callipers and are provided in Table 1.

105

Figure 1. The geologic map showing the quarry where *Dianmeisaurus mutaensis* sp. nov. (HFUT MT-21-08-001) was discovered (updated after Hu & Liu, 2022). Abbreviations: E, Palaeogene; T_{2-3f}, Falang Formation, Ladinian-Carnian, Middle-Late Triassic; T_{2y}, Yangliujing Formation, Anisian-Ladinian, Middle Triassic; T_{2g}², Upper Member of Guanling Formation, Anisian, Middle Triassic; T_{2g}¹, Lower Member of Guanling Formation, Anisian, Middle Triassic; T₁, Lower Triassic.

Systematic palaeontology

Sauropterygia Owen, 1860

Eosauropterygia Rieppel, 1994

Pachypleurosauria Nopcsa, 1928

Dianmeisaurus Shang & Li, 2015

Revised diagnosis

Postfrontal with a distinct constriction behind the orbit (also present in *Anarosaurus*, *Honghesaurus*, and *Prosantosaurus*); distal end of sacral ribs distinctly expanded (also present in *Diandongosaurus* and *Qianxisaurus*); interorbital septum extremely narrowed and distinctly shorter than the distance between external nares (a synapomorphy of *Dianmeisaurus*); skull table with deeply concave posterior margin (also present in *Dawazisaurus* and *Diandongosaurus*).

124 *Dianmeisaurus mutaensis* sp. nov.

125 *Holotype*

126 HFUT MT-21-08-001, a complete and articulated skeleton exposed in dorsal view
127 (part and counterpart).

128 *Ontogenetic evaluation*

129 There are currently three known specimens of *Dianmeisaurus*, among which HFUT
130 MT-21-08-001 represents the smallest individual with a total body length of 99.2 mm.
131 It is much smaller than the two published specimens of *Dianmeisaurus gracilis* (315
132 mm for the holotype, see Shang & Li, 2015; 250 mm for IVPP V 17054, see Shang et
133 al., 2017). Several morphological characters indicate that HFUT MT-21-08-001 is
134 skeletally immature. First, the skull is poorly ossified. The skull has fontanelles,
135 which generally indicates that the individual is at an early ontogenetic stage (Lin &
136 Rieppel, 1998; Piñeiro et al., 2012; Rieppel, 1992a, 1992b; Rieppel, 1993a; Wise et
137 al., 2009). Secondly, the distal end of the humeri is incompletely ossified since the
138 entepicondylar groove is still present. The entepicondylar groove starts close and
139 turns into a foramen when the individual becomes more mature (Currie & Carroll,
140 1984; Sander, 1989). Thirdly, among the carpals and tarsals of HFUT MT-21-08-001,
141 only the astragalus is ossified, also indicating an early ontogenetic stage of the
142 individual (Fröbisch, 2008; Rieppel, 1992b; Sander, 1989). All these lines of evidence
143 strongly support the conclusion that HFUT MT-21-08-001 is skeletally immature.

Type Locality

Muta Village, Luxi County, Yunnan Province, China.

Type Horizon

Upper Member of Guanling Formation, Anisian, Middle Triassic.

Etymology

Named after Muta village where the holotype was collected.

Diagnosis

A pachypleurosaur with following autapomorphies among pachypleurosaurs: 23 cervical vertebrae, 20 dorsal vertebrae, and two sacral vertebrae; postfrontal extending posteriorly to a level beyond the middle of parietal; last dorsal rib stout and shorter than the first sacral rib; phalangeal formula of manus and pes 2-3-4-4-2 and 1-2-3-4-3 respectively. In addition to the above mentioned autapomorphies, *Dianmeisaurus mutaensis* also differs from *D. gracilis* in the following morphological characters: maxilla enters the external naris; anterior process of the frontal does not extend beyond the anterior margin of the orbit; postfrontal excluded from the upper temporal fenestra; coronoid process absent.

Figure 2. The holotype of *Dianmeisaurus mutaensis* sp. nov. (HFUT MT-21-08-001). A. the skeleton in dorsal view; B, the counterpart of A (natural mold). Scale bars equal 1 cm.

Description

The skeleton, embedded in the dark-grey micritic limestone, consists of a part and its counterpart. The specimen is well-preserved, with a total length of 99.2 mm. Adjacent to the specimen, there are scattered limb and rib bones from other individual(s), but the limited information available prevents further identification.

Skull

The skull of HFUT MT-21-08-001 is dorsoventrally compressed and slightly distorted (Fig. 3). The surface of the dermatocranial bones shows weak sculpturing. The preorbital region of the skull is slightly shorter than the postorbital region. The snout is very short and round anteriorly. The occipital portion is plate-like without an occipital crest.

Figure 3. The skull of *Dianmeisaurus mutaensis* sp. nov. (HFUT MT-21-08-001). A. photo; B, interpreted drawing. Abbreviations: an, angular; ar, articular; ata, atlas arch; atc, atlas centrum; axc, axial centrum; bo, basioccipital; c3, 3rd cervical centrum; d, dentary; eo-op, exoccipital-opisthotic complex; f, frontal; fo, fontanelle; j, jugal; m, maxilla; n, nasal; p, parietal; par, prearticular; pm, premaxilla; po, postorbital; pof, postfrontal; prf, prefrontal; q, quadrate; r3, 3rd cervical rib; sa, surangular; so, supraoccipital; sq, squamosal. The red arrow marks the pit on the premaxilla-maxilla suture. Scale bars equal 1 mm.

Table 1. Measurements of *Dianmeisaurus mutaensis* sp. nov. (HFUT MT-21-08-001).

MEASUREMENT	VALUE (MM)
Body length	99.2
Condylbasal skull length	10.7
Length of skull (to posterior margin of the parietal	9.3

Maximum width of the skull	8.2
Diameter of right external naris (longitudinal×transverse)	0.5×0.8
Minimum width between external nares	0.5
Diameter of right orbit (longitudinal×transverse)	3.8×3.3
Minimum width between orbits	0.3
Diameter of pineal foramen	0.3
Distance from snout tip to anterior margin of external naris	0.9
Distance from snout tip to anterior margin of orbit (preorbital region)	3.0
Minimum distance between external naris and orbit (length from the posterior margin of the external naris to the anterior margin of the orbit)	1.6
Distance from snout tip to anterior margin of upper temporal fenestra	7.0
Minimum distance between orbit and upper temporal fenestra (minimum width of the postorbital arch)	0.4
Distance from posterior margin of orbit to the posterolateral end of the squamosal (postorbital region)	3.4
Length of right humerus	4.7
Proximal width of right humerus	1.4
Distal width of right humerus	1.5
Minimal width of right humerus	0.9
Length of left ulna	2.6
Length of left radius	3.0
Proximal width of left ulna	0.7
Distal width of left ulna	0.6
Proximal width of left radius	0.8
Distal width of left radius	0.5
Length of left femur	6.6
Proximal width of left femur	1.6
Distal length of left femur	1.1
Minimal width of left femur	0.9
Length of right tibia	3.2

Minimal width of right tibia	0.5
Length of right fibula	3.0
Minimal width of right tibia	1.0

184 The paired premaxillae constitute the short snout in front of the external nares and
185 the anterior margin of the external nares. The posterodorsal processes of the
186 premaxilla extend backward along the midline, separating the anterior part of the
187 nasal. Each posterolateral process of the premaxilla contacts the maxilla around the
188 lateral margin of the external naris, where the snout constriction is absent as in most
189 pachypleurosaurs (Rieppel, 2000), but a depression is developed.

190 The maxilla forms the anterolateral margin of the orbit. The anterior process of the
191 maxilla runs into the lateral corner of the external naris where it contacts the
192 premaxilla. Dorsally, the ascending process of the maxilla is wedged between the
193 nasal anteromedially and the prefrontal posteromedially. It almost reaches the level of
194 the midpoint of the anterior margin of the orbit. A small pit is located at the maxilla-
195 prefrontal suture, which is close to the anterolateral corner of the orbit. The posterior
196 process of the maxilla abuts the lateral margin of the jugal and reaches the posterior
197 margin of the orbit.

198 The external naris is located anteriorly, quite close to the tip of the snout, as is also
199 the case in *Dianmeisaurus gracilis* and *Panzhousaurus* (Jiang et al., 2019). The length
200 from the tip of the snout to the anterior margin of the external naris divided by the
201 condylobasal skull length is 0.08. The longitudinal diameter of the external naris is

202 less than its transverse diameter and the longitudinal diameter of the orbit. The lateral
203 corner of the external naris shows an acute angle.

204 A pair of roughly triangular nasal bones meet along the midline, with the contact
205 length comprising 3/4 of the total nasal length. Anteriorly, the nasal forms the
206 posterior and part of the dorsal margin of the external naris. Anterodorsally, the
207 paired nasals embrace the posterior processes of the premaxillae. Anterolaterally,
208 the nasals are not well ossified, leaving an open gap with the maxilla and
209 prefrontal. This gap is interpreted as a morphological feature related to the early
210 ontogenetic stage of the specimen, i.e. a fontanelle. The posterior processes of the
211 nasal separate the posterior processes of the prefrontal and taper backward to
212 overlie the frontal, almost reaching the midpoint of the medial margin of the orbit,
213 which is an autapomorphy of the species. The surface of the nasal shows a few
214 deep pits.

215 The circular orbit is large, about twice longer than the upper temporal fenestra. The
216 interorbital septum is extremely narrow. The minimum width of the interorbital
217 septum is distinctly shorter than the minimum distance between the external nares, a
218 synapomorphy of *Dianmeisaurus*. The prefrontal forms the anterodorsal margin of the
219 orbit. Laterally, the prefrontal contacts the maxilla. The posterior process of the
220 prefrontal meets the frontal. The paired frontals form the dorsal margin of the orbit.
221 The anterior process of the frontal almost extends to the midpoint of the medial
222 margin of the orbit, which is convergently present in *Dianopachysaurus* among

223 pachypleurosaurs (Liu et al., 2011). The anterior process of the frontal in other
 224 pachypleurosaurs extends very close to or beyond the anterior margin of the orbit
 225 (e.g., Cheng et al., 2016; Klein et al., 2022; Shang et al., 2011; Jiang et al., 2019; Xu
 226 et al., 2022). The well-developed posterolateral processes of the frontals are widely
 227 separated from the upper temporal fenestra and enter between the postfrontal and
 228 parietal.

229 The postfrontal forms the posterodorsal margin of the orbit. It has a roughly
 230 triradiate shape. The lateral margin of the postfrontal is distinctly constricted, which is
 231 also present in *Dianmeisaurus gracilis*, *Anarosaurus*, *Honghesaurus*, and
 232 *Prosantosaurus* among pachypleurosaurs (Klein, 2009; Klein et al., 2022; Shang et
 233 al., 2017; Xu et al., 2022). The postfrontal is separated from the upper temporal
 234 fenestra by the postorbital and parietal, which is otherwise only seen in *Honghesaurus*
 235 (Xu et al., 2022) among pachypleurosaurs. The posterior process of the postfrontal is
 236 embraced by the parietal and extends beyond the midpoint of the skull table, a
 237 synapomorphy shared with *Panzhousaurus* (Jiang et al., 2019) among
 238 pachypleurosaurs.

239 The postorbital defines the lateral and the entire anterior margin of the upper
 240 temporal fenestra. The lateral process of the postorbital contacts the jugal. The dorsal
 241 process of the postorbital narrowly meets the parietal, separating the postfrontal from
 242 the upper temporal fenestra. The posterior process of the postorbital contacts the
 243 squamosal with an interdigitated suture.

1 244 The boomerang-shaped jugal constitutes the posterolateral corner of the orbit. The
2
3
4 245 ventral margin of the jugal contacts the maxilla. The posterodorsal process of the
5
6 246 jugal covers the postorbital, being separated from the squamosal by the postorbital.
7
8

9 247 The parietals are partly fused. A distinct suture is present in front of the pineal
10
11
12 248 foramen, dividing the paired parietals, but the parietal is fully fused behind the
13
14
15 249 pineal foramen. The parietal is very broad. Anteriorly, the interdigitated parietal-
16
17
18 250 frontal suture is located anterior to the posterior margin of the orbit. A large
19
20
21 251 unossified gap between the frontal and parietal indicates the existence of another
22
23
24 252 fontanelle. Laterally, the parietal constitutes the posterodorsal margin of the upper
25
26
27 253 temporal fenestra. Posteriorly, the parietal contacts the squamosal and the
28
29
30 254 supraoccipital. The circular pineal foramen is in the middle of the parietal table.
31

32 255 Due to the postmortem alteration, the right upper temporal fenestra is completely
33
34
35 256 covered by the right squamosal, and the left fenestra is incomplete. Even so, it is
36
37
38 257 conclusive that the upper temporal fenestra is distinctly shorter than the orbit.
39

40 258 The large squamosal is irregular in shape due to its postmortem alteration. The
41
42
43
44 259 forked anterior process of the squamosal forms half of the supratemporal arch. The
45
46
47 260 lateral process of the squamosal caps the quadrate. Medially, the squamosal
48
49
50 261 contacts the dorsal margin of the supraoccipital.
51

52 262 The quadrate is partially covered by the squamosal. The condylar portion of the
53
54
55 263 left quadrate is exposed in lateral view. The quadrate shows a concave region on
56
57
58 264 the right side of the skull.
59
60
61
62
63
64
65

265 The supraoccipital is exposed horizontally without a medial crest. The
 266 supraoccipital contacts the parietal anteriorly with a V-shaped suture and the
 267 squamosal laterally. Posteriorly, it meets the exoccipital-opisthotic complex. The
 268 basioccipital is located at the same level as the mandibular articulations.

269 The relationships between bones of the lower jaw are indeterminate due to the poor
 270 preservation of the exposed surface. However, a coronoid process is certainly absent,
 271 which is different when compared to *Dianmeisaurus gracilis*, *Diandongosaurus* and
 272 *Keichousaurus* (Holmes et al., 2008; Shang et al., 2011; Shang et al., 2017). The
 273 dentary extends posteriorly to the midpoint of the orbit and contacts the angular.
 274 Medially, the angular meets the surangular. Both of them contribute to the lateral and
 275 dorsal margins of the lower jaw. The articular shows a distinct trough in dorsal view,
 276 forming the dorsal part of the well-developed retroarticular process. The prearticular is
 277 disarticulated from the articular and constitutes the floor of the retroarticular process.

278 The dentition of the right side is better preserved than the dentition of the left side.
 279 Thus, the following description is based on the dentition of the right side. All teeth
 280 have a pointed apex. Two premaxillary teeth are visible and are similar in size. No
 281 premaxillary and maxillary fangs are present. Five maxillary teeth are visible, of
 282 which the second is distinctly smaller than the others, likely because it represents a
 283 replacement tooth.

284 *Postcranial skeleton*

285 *Vertebrae*

286 HFUT MT-21-08-001 comprises 23 cervical vertebrae, 20 dorsal vertebrae, only two
287 sacral vertebrae, and at least 40 caudal vertebrae (Fig. 2). All zygapophyses are
288 pachyostotic and no intercentra are present. The atlas is dislocated and covered by the
289 basioccipital. Two triangular atlas arches are disarticulated and well exposed (Fig. 3).
290 The cervical vertebrae have low neural spines. The neural spines of the dorsal region
291 are also low, and there is no elongated transverse process on the dorsal region. The
292 caudal vertebrae become smaller posteriorly.

293 *Ribs*

294 The ribs are slender (Fig. 2). The distal end of the dorsal rib becomes flat and slightly
295 expanded. The first dorsal rib is almost twice as long as the last cervical rib. The last
296 (20th) dorsal rib is short and robust. It is shorter than the sacral ribs and all other
297 dorsal ribs, which represents an autapomorphy of the species among
298 Pachypleurosauria. The distal end of last dorsal rib shows an expansion that is slightly
299 more obvious than the distal expansion of other dorsal ribs. However, the last dorsal
300 ribs are too short to articulate with the ilium and do not extend toward the ilium.
301 Additionally, there is no evidence of dislocation for the last dorsal ribs (Fig. 6). So
302 they can not be sacral ribs, but at the best be called transitional ribs (Romer, 1956).
303 The left side of the sacral ribs are completely exposed (Fig. 6). The distal end of the
304 sacral ribs is slightly expanded. The slender caudal ribs all taper to a point. The first

caudal rib extends perpendicularly to the body axis. The third caudal rib is the longest among all caudal ribs. From the third caudal rib to the sixth, the length of the caudal rib is reducing gradually. The 1st-6th caudal ribs of this specimen are prominent. In *Dianmeisaurus gracilis*, the 1st-9th caudal ribs are prominent, while in *Panzhousaurus*, prominent caudal ribs are present on 1st-11th caudal vertebrae.

Pectoral girdle

Among the pectoral girdle elements (Fig. 4), the interclavicle and coracoid are completely covered by ribs and vertebrae. The left scapula is exposed in the lateral view, while the right scapula is exposed in the medial view. As in all other sauropterygians (Klein et al., 2022; Rieppel, 2000), the posterior margin of the clavicle is connected to the medial surface of scapula, a synapomorphy of sauropterygians. The posteriorly directed dorsal wing of the scapula is rod-like and tapers to a blunt tip, a synapomorphy of eosauroptrygians (Rieppel, 2000).

318

Figure 4. Pectoral region of *Dianmeisaurus mutaensis* sp. nov. (HFUT MT-21-08-001). A. photo; B, interpreted drawing. Abbreviations: cl, clavicle; cv23, 23rd cervical vertebra; dv1, 1st dorsal vertebra; h, humerus; sc, scapula. Scale bars equal 1 mm.

Forelimb

The right forelimb is preserved completely (Fig. 5). The humerus is curved as in all sauropterygians. Owing to the weakly developed deltopectoral crest, the preaxial margin of the humerus is slightly angulated. The distal end of the humerus is slightly broadened. Due to its early ontogenetic stage, an entepicondylar groove can be seen in

1 327 this specimen, instead of the entepicondylar foramen (Sander, 1989). The ulna is
2
3
4 328 shorter than the radius. The preaxial margin of the ulna is smoothly concave. Both
5
6 329 ends of the ulna are slightly expanded. The radius is straight, with its proximal part
7
8
9 330 slightly wider than the distal end. The proximal end and mid-shaft of the radius are
10
11
12 331 approximately as broad as those of the ulna.
13

14
15 332 No carpal element is ossified. Metacarpal 1 is distinctly shorter and stouter than
16
17
18 333 metacarpals 2- 4, of which metacarpal 3 is the longest. The phalangeal elements are
19
20
21 334 tightly connected. The phalangeal formula of the manus is 2-3-4-4-2.
22

23
24 335
25
26 336 **Figure 5.** Right forelimb of *Dianmeisaurus mutaensis* sp. nov. (HFUT MT-21-08-001). A.
27 337 photo; B, interpreted drawing. Abbreviations: d, digit; eng, entepicondylar groove; h,
28
29 338 humerus; r, radius; sc, scapula; u, ulna. Scale bars equal 1 mm.
30

31 339 *Pelvic girdle*

32
33
34 340 The pelvic girdle is partially exposed in dorsal view (Fig. 6). The dorsal blade of the
35
36
37 341 ilium is reduced to a simple stub. The pubis and ischium are flat bones, thickened
38
39
40 342 dorsoventrally at the lateral margin. The ischium shows the concave postaxial margin.
41

42
43 343
44
45 344 **Figure 6.** Sacral region of *Dianmeisaurus mutaensis* sp. nov. (HFUT MT-21-08-001). A.
46 345 photo; B, interpreted drawing. Abbreviations: cav, caudal vertebra; dr, dorsal rib; dv, dorsal
47
48 346 vertebra; fi, fibula; il, ilium; is, ischium; pu, pubis; sr, sacral rib; sv, sacral vertebra. Scale
49
50 347 bars equal 1 mm.
51

Hindlimb

The hind limb is well preserved except for the distal portion of the left femur (Fig. 2).

The femur is long and sigmoidally curved, and the ratio of femur length divided by humerus length is 1.39. The anterior and posterior femoral condyles are subequally extended. The internal trochanter is absent. The fibula and tibia are equal in length, but the flat tibia is much more broadened than the fibula. The small round astragalus is the only ossified tarsal bone. Metatarsal 1 is the shortest and stoutest element of the metatarsals, while others are long and slender. Metatarsals 3 and 4 are approximately the same length, slightly longer than metatarsals 2 and 5. The phalangeal formula of the pes is 1-2-3-4-3.

Figure 7. Right hindlimb of *Dianmeisaurus mutaensis* sp. nov. (HFUT MT-21-08-001). A. photo; B, interpreted drawing. Abbreviations: as, astragalus; d, digit; f, femur; fi, fibula; il, ilium; ti, tibia. Scale bars equal 1 mm.

Phylogenetic analysis

Figure 8. Strict consensus tree showing phylogenetic relationships of eosauropterygians. Bootstrap values over 50% (with 1000 replicates) are indicated in the tree.

To assess the phylogenetic position of *Dianmeisaurus mutaensis* among eosauropterygians, we compiled a new data matrix consisting of 203 characters, among which 182 are informative, for 43 taxa. The matrix was based on a revised version of the one presented by Li and Liu (2020), and many new characters were

372 added through a comparative study. We also coded several new taxa of
373 eosauropterygians discovered in recent years, including *Qianxisaurus* (Cheng et al.,
374 2012), *Odoiporosaurus* (Renesto et al., 2014), *Dianmeisaurus* (Shang & Li, 2015;
375 Shang et al., 2017), *Dawazisaurus* (Cheng et al., 2016), *Panzhousaurus* (Jiang et al.,
376 2019; Lin et al., 2021), *Honghesaurus* (Xu et al., 2022), and *Prosantosaurus* (Klein et
377 al., 2022). In our phylogenetic analysis, Araeoscelidia, Younginiformes,
378 Archosauromorpha, and *Placodus* were still selected as outgroups taxa as in Li and
379 Liu (2020).

380 Heuristic searches of the new data matrix found five most parsimonious trees (tree
381 length = 811, consistency index = 0.3169, retention index = 0.6139). *Dianmeisaurus*
382 *mutaensis* forms the sister group to *D. gracilis*. The strict consensus tree recovered
383 *Dianmeisaurus* as the sister group to *Panzhousaurus*. The clade consisting of
384 *Dianmeisaurus* and *Panzhousaurus* occupies the basal-most position of
385 Pachypleuroosauria (Fig. 8). Meanwhile, the monophyly of Eusauropterygia is
386 collapsed. Pistosauroidea, *Majiashanosaurus*, and *Hanosaurus* constitute the
387 consecutive sister group to a monophyletic clade including Pachypleuroosauria and
388 Nothosauroidea. Our phylogenetic analysis recovered a monophyletic
389 Pachypleuroosauria clade, which is supported by six unambiguous synapomorphies:
390 bones in the dermatocranium relatively smooth (character 1: 1); the ratio of
391 longitudinal diameter of upper temporal divided by that of orbit is between 0.5-1
392 (character 45: 2); presence of a trough on the dorsal surface of retroarticular process

393 (character 82: 1); anterolaterally expanded corners of clavicles present (character 128:
394 1); anterior preaxial margin of shaft of radius rather straight (character 190: 2); pes
395 ungual phalanges extremely expanded (character 194: 1).

396 **Discussion**

397 *Comparison with Dianmeisaurus gracilis*

398 HFUT MT-21-08-001 is identified as a pachypleurosaur because of the presence of
399 the following characteristics: the upper temporal fenestra distinctly smaller than the
400 orbit, an anteriorly extended jugal that enters the ventral margin of the orbit, a distinct
401 trough on the dorsal surface of the retroarticular process, pachyostotic pre- and
402 postzygapophyses, and the reduced dorsal iliac blade. HFUT MT-21-08-001 also
403 shares several derived characters with *Dianmeisaurus gracilis*: the postfrontal with
404 distinct constriction behind the orbit; the width of interorbital septum distinctly
405 shorter than the minimum length between external naris; the posterior margin of skull
406 table deeply concave; the distal head of sacral ribs expanded.

407 Nevertheless, HFUT MT-21-08-001 shows many differences when compared with
408 *Dianmeisaurus gracilis*. In *Dianmeisaurus gracilis*, the postnarial process of the
409 premaxilla excludes the maxilla from the external naris, whereas in HFUT MT-21-08-
410 001, the maxilla enters the external naris, which is similar to all other
411 pachypleurosaurs (Rieppel., 2000; Cheng et al., 2012; Klein et al., 2022; Renesto et
412 al., 2014; Liu et al., 2011; Shang et al., 2011; Cheng et al., 2016). Also, the

413 postfrontal extends backward beyond the frontal to a level close to the middle of the
 414 skull table in HFUT MT-21-08-001, a unique morphology among pachypleurosaurs,
 415 while it just reaches the posterior end of the frontal in *Dianmeisaurus gracilis*. Also,
 416 the postfrontal is excluded from the margin of the upper temporal fenestra in HFUT
 417 MT-21-08-001, but the postfrontal of *Dianmeisaurus gracilis* enters the upper
 418 temporal fenestra. Contrary to the presence of a distinct coronoid process in
 419 *Dianmeisaurus gracilis*, the coronoid process in HFUT MT-21-08-001 is absent.

420 There are even more differences in the postcranial morphology between HFUT
 421 MT-21-08-001 and *Dianmeisaurus gracilis*. In contrast to the long and slender last
 422 dorsal rib in *Dianmeisaurus gracilis*, HFUT MT-21-08-001 has a stout last dorsal rib
 423 that is shorter than the first sacral rib. The most significant difference is the number of
 424 sacral vertebrae, which is four in *Dianmeisaurus gracilis* but only two in HFUT MT-
 425 21-08-001. The phalangeal formula of the manus of HFUT MT-21-08-001 is 2-3-4-4-
 426 2 and that of the pes is 1-2-3-4-3, which are both less than the number of phalanges in
 427 *Dianmeisaurus gracilis* (manus: 2-3-5-5-3(?), pes: 2-3-4-5-5(?)).

428 Although HFUT MT-21-08-001 is a juvenile, these differences do not change
 429 during the development of the individual among reptiles, as far as we know (Currie,
 430 1981; Currie & Carroll, 1984; Delfino & Sanchez-Villagra, 2010; Fröbisch, 2008;
 431 Griffin et al., 2021; Lin & Rieppel, 1998; Rieppel, 1992b; Rieppel, 1993a; Rieppel,
 432 1993b; Rieppel, 1994; Sander, 1989). Therefore, we erected a new species for HFUT
 433 MT-08-001, i.e., *Dianmeisaurus mutaensis* sp. nov..

Phylogenetic implications to the interrelationships of eosauropterygians
 Many eosauropterygian phylogenies were published after the comprehensive
 review of sauropterygians by Rieppel (2000). These phylogenetic analyses
 accompanied the description of *Dawazisaurus* (Cheng et al., 2016),
Diandongosaurus (Liu et al., 2021; Liu et al., 2015; Sato et al., 2014a; Shang et al.,
 2011), *Dianmeisaurus* (Shang & Li, 2015; Shang et al., 2017), *Dianopachysaurus*
 (Liu et al., 2011), *Honghesaurus* (Xu et al., 2022), *Luopingsaurus* (Xu et al., 2023),
Majiashanosaurus (Jiang et al., 2014), *Odoiporosaurus* (Renesto et al., 2014),
Panzhousaurus (Jiang et al., 2019; Lin et al., 2021), *Prosantosaurus* (Klein et al.,
 2022), *Qianxisaurus* (Cheng et al., 2012), and *Yunguisaurus* (Cheng et al., 2006;
 Lu et al., 2021; Sato et al., 2010, 2014b; Shang et al., 2016; Wang et al., 2019;
 Zhao et al., 2008). But most of these phylogenetic analyses relied on the data
 matrix of Rieppel et al. (2002) or slightly modified versions. Recently, some novel
 data matrices for analyzing the interrelationship of eosauropterygians have been
 constructed to incorporate the morphological information available from new
 Chinese eosauropterygians (Li & Liu, 2020; Lin et al., 2021; Xu et al., 2023). In Li
 and Liu (2020), the monophyly of Eusauropterygia collapsed, and
 Pachypleurosauria and Nothosauroida constituted an unnamed clade. Our new
 phylogenetic analysis here also shows the collapse of the monophyly of
 Eusauropterygia, as in Li and Liu (2020), and suggests a new monophyletic clade
 comprising Pachypleurosauria and Nothosauroida. Pistosauroida,

455 *Majiashanosaurus*, and *Hanosaurus* comprise the consecutive sister groups of the
 456 new clade. These results are consistent with those of Li and Liu (2020). However,
 457 the Early Triassic *Corosaurus* occupies the basal-most position of the
 458 Pistosauroidea in this study, as traditionally recognized (Rieppel 2000). This is in
 459 contrast to the phylogenetic result of Li and Liu (2020), which shows *Corosaurus*
 460 as the most basal member of Eosauropterygia. *Hanosaurus* is recovered in a
 461 relatively basal position within Eosauropterygia as in some previous analyses (e.g.,
 462 Jiang et al., 2019; Li & Liu, 2020; Liu et al., 2015; Ma et al., 2015; Shang et al.,
 463 2017; Xu et al., 2022), rather than in a lineage leading to the Nothosauroidea (e.g.,
 464 Cheng et al., 2012; Jiang et al., 2014; Sato et al., 2014a; Shang & Li, 2015), as a
 465 basal pachypleurosaur (e.g., Neenan et al., 2015), or even outside of the
 466 Sauropterygia clade (e.g., Cheng et al., 2016; Klein & Scheyer, 2014; Marquez-
 467 Aliaga et al., 2019; Neenan et al., 2013).

468 *Monophyly and the palaeobiogeographic origin of Pachypleurosauria*

469 The first cladistic analysis to test the monophyly of Pachypleurosauria was conducted
 470 by Storrs (1991). The monophyly of Pachypleurosauria was subsequently confirmed
 471 by a series of independent studies (reviewed in Rieppel, 2000). However, Holmes et
 472 al. (2008) restudied *Keichousaurus hui* and questioned the monophyly of
 473 Pachypleurosauria for the first time, which has been supported by several subsequent
 474 studies (e.g., Cheng et al., 2016; Jiang et al., 2014; Marquez-Aliaga et al., 2019;

Shang et al., 2011; Wu et al., 2011). Nevertheless, some other studies still support the traditional view that Pachypleurosauria is monophyletic (e.g., Liu et al., 2011; Neenan et al., 2013).

A monophyletic Pachypleurosauria is also recovered here, as in several recent studies (Li & Liu, 2020; Lin et al., 2021; Liu et al., 2021). However, different from the traditional topology where *Dianmeisaurus* forms the sister group of *Diandongosaurus*, *Dianmeisaurus* forms the sister group of *Panzhousaurus*, and together they occupy the basal-most position of Pachypleurosauria in this study. *Dianopachysaurus* forms a monophyletic clade with *Dawazisaurus*, which comprises the sister group to all remaining pachypleurosaurs. *Keichousaurus* and *Diandongosaurus* form a monophyletic clade, comprising the sister group to a clade consisting of all European pachypleurosaurs. Our result further indicates that two middle Anisian pachypleurosaurs from South China, *Qianxisaurus* and *Honghesaurus*, are deeply nested in the European pachypleurosaurs, similar to the results of Xu et al. (2022, 2023). Compared with other Chinese pachypleurosaurs, *Qianxisaurus* and *Honghesaurus* exhibit some derived characters: the snout is elongated; the ratio of the longitudinal diameters of the upper temporal divided by that of the orbit is less than 0.5; the deltopectoral crest is well-developed; the posterior process of the postfrontal is close to the middle of the skull table.

Our phylogenetic analysis indicates that Chinese pachypleurosaurs, with the exception of *Qianxisaurus* and *Honghesaurus*, comprise the consecutive sister

groups to all European pachypleurosaurs, supporting a hypothesis that Pachypleurosauria originated in the eastern Tethys (Liu et al., 2011; Renesto et al., 2014; Rieppel & Lin, 1995). However, the earliest known pachypleurosaurs, *Dactylosaurus*, is from the early Anisian of the Germanic Basin (Rieppel & Hagdorn, 1997), which implies the existence of a ghost lineage in the eastern Tethys. The two unnamed pachypleurosaurs from Myanmar (San et al., 2019), which could potentially be the oldest known pachypleurosaurs, could falsify the existence of a ghost lineage. However, the geological age in the region where the Myanmar pachypleurosaurs were collected still requires further study.

Conclusion

Dianmeisaurus mutaensis sp. nov. is established based on a newly discovered specimen from Muta village, Luxi county, Yunnan Province, China. *Dianmeisaurus mutaensis* exhibits several automorphic features, including the postfrontal extending posteriorly to the middle of the parietal table and being excluded from upper temporal fenestra, a stout last dorsal rib shorter than the first sacral rib, and two sacral vertebrae.

In addition, a novel data matrix was compiled to re-evaluate the interrelationships of eosauropterygians. Phylogenetic analysis shows the collapse of the monophyly of Eusauropterygia. Pistosauroidea, *Majiashanosaurus*, and *Hanosaurus* constitute the consecutive sister groups to a monophyletic clade comprising Pachypleurosauria and

1 516 Nothosauroidae. Furthermore, the monophyly of Pachypleurosauria is supported by
2
3 517 six synapomorphies. Our phylogenetic results provide further evidence to the eastern
4
5
6 518 Tethys origin of pachypleurosaurs. However, early Anisian pachypleurosaurs from
7
8
9 519 the eastern Tethys region are required to test the biogeographic hypothesis.
10
11
12

13 520 **Institutional Abbreviations**

14
15

16 521 HFUT, Hefei University of Technology, Hefei, Anhui, China; IVPP, Institute of
17
18
19 522 Vertebrate Paleontology and Paleoanthropology, Chinese Academy of Sciences in
20
21
22 523 Beijing, China.
23
24

25 524 **Declarations**

26
27
28

29 525 ***Availability of data and materials***

30
31

32 526 All data generated or analyzed during this study are included in the Supplementary
33
34
35 527 Data of this published article. HFUT MT-21-08-001 is stored at the Geological
36
37
38 528 Museum of HFUT, Hefei, China, and publically accessed.
39
40

41 529 ***Competing interests***

42
43

44 530 The authors declare that they have no competing financial interests.
45
46

47 531 ***Funding***

48
49
50

51 532 This work was supported by the National Natural Science Foundation of China under
52
53
54 533 Grant numbers 42172026 and 41772003.
55
56
57
58
59
60
61
62
63
64
65

1 534 ***Author's contributions***

2
3 535 JL designed the research. YWH prepared all figures and tables. QL and YWH
4
5
6 536 compiled the new data matrix, and YWH performed phylogenetic analyses. YWH and
7
8
9 537 JL were the major contributors to writing the manuscript. All authors read and
10
11
12 538 approved the final manuscript.
13
14

15 539 ***Acknowledgements***

16
17
18 540 We thank A. S. Wolniewicz for early discussions, S.P. Jiang, and other members from
19
20
21 541 the paleontological lab of HFUT for field assistance. We also acknowledge L. Y. Li
22
23
24 542 for preparing this specimen. The associate editor N. Klein, reviewer S.N.F. Spiekman
25
26
27 543 and another anonymous reviewer provided very helpful comments that significantly
28
29
30 544 improved the manuscript.
31
32
33

34 545 **Reference**

35
36
37 546 Čerňanský, A., Klein, N., Soták, J., Olšavský, M., Šurka, J., & Herich, P. (2018). A
38
39
40 547 Middle Triassic pachypleurosauro (Diapsida: Eosauropterygia) from a restricted
41
42
43 548 carbonate ramp in the Western Carpathians (Gutenstein Formation, Fatric Unit):
44
45
46 549 paleogeographic implications. *Geologica Carpathica*, 69(1), 3-16.
47
48
49 550 Cheng, Y. N., Sato, T., Wu, X. C., & Li, C. (2006). First complete pistosauroid from
50
51
52 551 the Triassic of China. *Journal of Vertebrate Paleontology*, 26(2), 501-504.
53
54 552 [https://doi.org/10.1671/0272-4634\(2006\)26\[501:fcpftt\]2.0.co;2](https://doi.org/10.1671/0272-4634(2006)26[501:fcpftt]2.0.co;2)
55
56
57
58
59
60
61
62
63
64
65

- 553 Cheng, Y. N., Wu, X. C., Sato, T., & Shan, H.-Y. (2012). A new eosauropterygian
554 (Diapsida, Sauropterygia) from the Triassic of China. *Journal of Vertebrate*
555 *Paleontology*, 32(6), 1335-1349. <https://doi.org/10.1080/02724634.2012.695983>
- 556 Cheng, Y. N., Wu, X. C., Sato, T., & Shan, H.-Y. (2016). *Dawazisaurus brevis*, a new
557 eosauropterygian from the Middle Triassic of Yunnan, China. *Acta Geologica*
558 *Sinica - English Edition*, 90(2), 401-424. [https://doi.org/10.1111/1755-](https://doi.org/10.1111/1755-6724.12680)
559 6724.12680
- 560 Currie, P. J. (1981). *Hovasaurus boulei*, an aquatic eosuchian from the Upper Permian
561 of Madagascar. *Palaeontologia Africana*, 21, 99-168.
- 562 Currie, P. J., & Carroll, R. L. (1984). Ontogenetic changes in the eosuchian reptile
563 *Thadeosaurus*. *Journal of Vertebrate Paleontology*, 4(1), 68-84.
564 <http://www.jstor.org/stable/4522966>
- 565 Dalla Vecchia, F. M. (2006). A new sauropterygian reptile with plesiosaurian affinity
566 from the Late Triassic of Italy. *Rivista Italiana Di Paleontologia E Stratigrafia*,
567 112(2), 207-225. <Go to ISI>://000239397200003
- 568 de Miguel Chaves, C., Ortega, F., & Pérez-García, A. (2018). New highly
569 pachyostotic nothosauroid interpreted as a filter-feeding Triassic marine reptile.
570 *Biology Letters*, 14(8), 20180130. <https://doi.org/10.1098/rsbl.2018.0130>
- 571 de Miguel Chaves, C., Ortega, F., & Pérez-García, A. (2020). The Iberian Triassic
572 fossil record of Sauropterygia: an update. *Journal of Iberian Geology*, in press.
573 <https://doi.org/10.1007/s41513-020-00137-w>

- 574 Delfino, M., & Sanchez-Villagra, M. R. (2010). A survey of the rock record of
575 reptilian ontogeny. *Seminars in Cell & Developmental Biology*, 21(4), 432-440.
576 [http://www.sciencedirect.com/science/article/B6WX0-4XNN5NC-](http://www.sciencedirect.com/science/article/B6WX0-4XNN5NC-3/2/499553de82dee9854ed8866212f5b39f)
577 [3/2/499553de82dee9854ed8866212f5b39f](http://www.sciencedirect.com/science/article/B6WX0-4XNN5NC-3/2/499553de82dee9854ed8866212f5b39f)
- 578 Fröbisch, N. B. (2008). Ossification patterns in the tetrapod limb--conservation and
579 divergence from morphogenetic events. *Biological Reviews*, 83(4), 571-600.
580 <https://doi.org/10.1111/j.1469-185X.2008.00055.x>
- 581 Griffin, C. T., Stocker, M. R., Colleary, C., Stefanic, C. M., Lessner, E. J., Riegler,
582 M., Formoso, K., Koeller, K. & Nesbitt, S. J. (2021). Assessing ontogenetic
583 maturity in extinct saurian reptiles. *Biological Reviews*, 96(2),.
584 <https://doi.org/10.1111/brv.12666>
- 585 Holmes, R., Cheng, Y. N., & Wu, X. C. (2008). New information on the skull of
586 *Keichousaurus hui* (Reptilia: Sauropterygia) with comments on sauropterygian
587 interrelationships. *Journal of Vertebrate Paleontology*, 28(1), 76-84. <Go to
588 ISI>://000254408700008
- 589 Hu, Y. W., & Liu, J. (2022). A new morphotype of nothosaurs (Sauropterygia:
590 Nothosauridae) from the Middle Triassic of South China. *Historical Biology*, 1-
591 10. <https://doi.org/10.1080/08912963.2022.2122459>
- 592 Jiang, D. Y., Lin, W. B., Rieppel, O., Motani, R., & Sun, Z. Y. (2019). A new Anisian
593 (Middle Triassic) eosauroptrygian (Reptilia, Sauropterygia) from Panzhou,

594 Guizhou Province, China. *Journal of Vertebrate Paleontology*, 38(4), 1-9.

595 <https://doi.org/10.1080/02724634.2018.1480113>

596 Jiang, D. Y., Motani, R., Tintori, A., Rieppel, O., Chen, G. B., Huang, J. D., Zhang,
597 R., Sun, Z. Y. & Ji, C. (2014). The Early Triassic eosauropterygian
598 *Majiashanosaurus discocoracoidis*, gen. et sp. nov. (Reptilia, Sauropterygia),
599 from Chaohu, Anhui Province, People's Republic of China. *Journal of*
600 *Vertebrate Paleontology*, 34(5), 1044-1052.

601 <https://doi.org/10.1080/02724634.2014.846264>

602 Jiang, D. Y., Motani, R., Hao, W. C., Rieppel, O., Sun, Y. L., Schmitz, L., & Sun, Z.
603 Y. (2008). First record of Placodontoidea (Reptilia, Sauropterygia, Placodontia)
604 from the Eastern Tethys. *Journal of Vertebrate Paleontology*, 28(3), 904-908.

605 <Go to ISI>://000259414500028

606 Kelley, N. P., Motani, R., Jiang, D. Y., Rieppel, O., & Schmitz, L. (2014). Selective
607 extinction of Triassic marine reptiles during long-term sea-level changes
608 illuminated by seawater strontium isotopes. *Palaeogeography,*
609 *palaeoclimatology, palaeoecology*, 400, 9-16.

610 <http://www.sciencedirect.com/science/article/pii/S0031018212004336>

611 Klein, N., Furrer, H., Ehrbar, I., Torres Ladeira, M., Richter, H., & Scheyer, T. M.
612 (2022). A new pachypleurosaur from the Early Ladinian Prosanto Formation in
613 the Eastern Alps of Switzerland. *Swiss J Palaeontol*, 141(1), 12.

614 <https://doi.org/10.1186/s13358-022-00254-2>

- 615 Klein, N., & Scheyer, T. M. (2014). A new placodont sauropterygian from the Middle
616 Triassic of the Netherlands. *Acta Palaeontologica Polonica*, 59(4), 887-902.
- 617 Li, Q., & Liu, J. (2020). An Early Triassic sauropterygian and associated fauna from
618 South China provide insights into Triassic ecosystem health. *Communications*
619 *Biology*, 3(1), 63. <https://doi.org/10.1038/s42003-020-0778-7>
- 620 Lin, K. B., & Rieppel, O. (1998). Functional morphology and ontogeny of
621 *Keichousaurus hui* (Reptilia, Sauropterygia). *Fieldiana (Geology) n.s.*, 39, 1-39.
- 622 Lin, W. B., Jiang, D. Y., Rieppel, O., Motani, R., Tintori, A., Sun, Z. Y., & Zhou, M.
623 (2021). Panzhousaurus Rotundirostris Jiang et al., 2019 (Diapsida:
624 Sauropterygia) and the Recovery of the Monophyly of Pachypleurosauridae.
625 *Journal of Vertebrate Paleontology*, e1901730.
626 <https://doi.org/10.1080/02724634.2021.1901730>
- 627 Liu, J., Rieppel, O., Jiang, D. Y., Aitchison, J. C., Motani, R., Zhang, Q. Y., Zhou, C.
628 Y. & Sun, Y. Y. (2011). A new pachypleurosaur (Reptilia, Sauropterygia) from
629 the lower Middle Triassic of SW China and the phylogenetic relationships of
630 Chinese pachypleurosaurs. *Journal of Vertebrate Paleontology*, 31(2), 292-302.
- 631 Liu, Q., Yang, T., Cheng, L., Benton, M. J., Moon, B. C., Yan, C., An, C. B. & Tian,
632 L. (2021). An injured pachypleurosaur (Diapsida: Sauropterygia) from the
633 Middle Triassic Luoping Biota indicating predation pressure in the Mesozoic. *Sci*
634 *Rep*, 11(1), 21818. <https://doi.org/10.1038/s41598-021-01309-z>

- 635 Liu, X. Q., Lin, W. B., Rieppel, O., Sun, Z. Y., Li, Z. G., Lu, H., & Jiang, D. Y.
636 (2015). A new specimen of *Diandongosaurus acutidentatus* (Sauropterygia)
637 from the Middle Triassic of Yunnan, China. *VERTEBRATA PALASIATICA*, in
638 *press*.
- 639 Ma, L. T., Jiang, D. Y., Rieppel, O., Motani, R., & Tintori, A. (2015). A new
640 pistosauroid (Reptilia, Sauropterygia) from the late Ladinian Xingyi marine
641 reptile level, southwestern China. *Journal of Vertebrate Paleontology*, 35(1),
642 e881832. <https://doi.org/10.1080/02724634.2014.881832>
- 643 Marquez-Aliaga, A., Klein, N., Reolid, M., Plasencia, P., Villena, J. A., & Martinez-
644 Perez, C. (2019). An enigmatic marine reptile, *Hispaniasaurus cranioelongatus*
645 (gen. et sp. nov.) with nothosauroid affinities from the Ladinian of the Iberian
646 Range (Spain). *Historical Biology*, 31(2), 223-233.
647 <https://doi.org/10.1080/08912963.2017.1359264>
- 648 Motani, R. (2009). The evolution of marine reptiles. *Evolution: Education and*
649 *Outreach*, 2(2), 224-235.
- 650 Neenan, J. M., Klein, N., & Scheyer, T. M. (2013). European origin of placodont
651 marine reptiles and the evolution of crushing dentition in Placodontia. *Nature*
652 *Communications*, 4, 1621. <http://dx.doi.org/10.1038/ncomms2633>
- 653 Neenan, J. M., Li, C., Rieppel, O., & Scheyer, T. M. (2015). The cranial anatomy of
654 Chinese placodonts and the phylogeny of Placodontia (Diapsida: Sauropterygia).

- 655 *Zoological Journal of the Linnean Society*, 175(2), 415-428.
- 656 <https://doi.org/10.1111/zoj.12277>
- 657 Piñeiro, G., Ferigolo, J., Ramos, A., & Laurin, M. (2012). Cranial morphology of the
- 658 Early Permian mesosaurid *Mesosaurus tenuidens* and the evolution of the lower
- 659 temporal fenestration reassessed. *Comptes Rendus Palevol*, 11(5), 379-391.
- 660 <https://doi.org/http://dx.doi.org/10.1016/j.crpv.2012.02.001>
- 661 Renesto, S., Binelli, G., & Hagdorn, H. (2014). A new pachypleurosaur from the
- 662 Middle Triassic Besano Formation of Northern Italy. *Neues Jahrbuch für*
- 663 *Geologie und Paläontologie - Abhandlungen*, 271(2), 151-168.
- 664 <https://doi.org/10.1127/0077-7749/2014/0382>
- 665 Rieppel, O. (1989). A new pachypleurosaur (Reptilia: Sauropterygia) from the Middle
- 666 Triassic of Monte San Giorgio, Switzerland. *Philosophical Transactions of the*
- 667 *Royal Society of London B*, 323(1212), 1-73.
- 668 <http://www.jstor.org/stable/2396749>
- 669 Rieppel, O. (1992a). The skull in a hatchling of *Sphenodon punctatus*. *Journal of*
- 670 *Herpetology*, 26(1), 80-84. <http://www.jstor.org/stable/1565028>
- 671 Rieppel, O. (1992b). Studies on skeleton formation in reptiles. I. The postembryonic
- 672 development of the skeleton in *Cyrtodactylus pubisulcus* (Reptilia: Gekkonidae).
- 673 *Journal of Zoology*, 227(1), 87-100. [https://doi.org/10.1111/j.1469-](https://doi.org/10.1111/j.1469-7998.1992.tb04346.x)
- 674 [7998.1992.tb04346.x](https://doi.org/10.1111/j.1469-7998.1992.tb04346.x)

- 675 Rieppel, O. (1993a). Studies on skeleton formation in reptiles. v. Patterns of
676 ossification in the skeleton of *Alligator mississippiensis* DAUDIN (Reptilia,
677 Grocodylia). *Zoological Journal of the Linnean Society*, 109(3), 301-325.
- 678 Rieppel, O. (1993b). Studies on skeleton formation in reptiles: patterns of ossification
679 in the skeleton of *Chelydra serpentina* (Reptilia, Testudines). *Journal of*
680 *Zoology*, 231(3), 487-509. <https://doi.org/10.1111/j.1469-7998.1993.tb01933.x>
- 681 Rieppel, O. (1994). Studies on skeleton formation in reptiles. Patterns of ossification
682 in the skeleton of *Lacerta agilis exigua* Eichwald (Reptilia, Squamata). *Journal*
683 *of Herpetology*, 28(2), 145-153. <http://www.jstor.org/stable/1564613>
- 684 Rieppel, O. (1999a). Phylogeny and paleobiogeography of Triassic Sauropterygia:
685 problems solved and unresolved. *Palaeogeography Palaeoclimatology*
686 *Palaeoecology*, 153(1-4), 1-15. <Go to ISI>://000082598100001
- 687 Rieppel, O. (1999b). The Sauropterygian genera *Chinchenia*, *Kwangsisaurus*, and
688 *Sanchiaosaurus* from the Lower and Middle Triassic of China. *Journal of*
689 *Vertebrate Paleontology*, 19(2), 321-337. <Go to ISI>://000084259200011
- 690 Rieppel, O. (Ed.). (2000). *Sauropterygia I* (Vol. 12A). Verlag Dr. Friedrich Pfeil.
- 691 Rieppel, O., & Hagdorn, H. (1997). Paleobiogeography of Middle Triassic
692 Sauropterygia in central and western Europe. In M. Callaway Jack & L. Nicholls
693 Elizabeth (Eds.), *Ancient Marine Reptiles* (pp. 121-144). Academic Press.

- 694 Rieppel, O., & Lin, K. (1995). Pachypleurosaurs (Reptilia: Sauropterygia) from the
695 Lower Muschelkalk, and a review of the Pachypleurosauroidea. *Fieldiana*
696 (*Geology*) *n.s.*, 32, 1-44.
- 697 Rieppel, O., Sander, P. M., & Storrs, G. W. (2002). The skull of the pistosaur
698 *Augustasaurus* from the Middle Triassic of northwestern Nevada. *Journal of*
699 *Vertebrate Paleontology*, 22(3), 577-592. <Go to ISI>://000178190800009
- 700 San, K. K., Fraser, N. C., Foffa, D., Rieppel, O., & Brusatte, S. L. (2019). The first
701 Triassic vertebrate fossils from Myanmar: Pachypleurosaurs in a marine
702 limestone. *Acta Palaeontologica Polonica*, 64(2), 357-362.
- 703 Sander, P. M. (1989). The pachypleurosaurids (Reptilia: Nothosauria) from the
704 Middle Triassic of Monte San Giorgio (Switzerland) with the description of a
705 new species. *Philosophical Transactions of the Royal Society of London B*,
706 325(1230), 561-666. <http://www.jstor.org/stable/2396911>
- 707 Sato, T., Cheng, Y. N., Wu, X. C., & Li, C. (2010). Osteology of *Yunguisaurus* Cheng
708 et al., 2006 (Reptilia; Sauropterygia), a Triassic pistosauroid from China
709 [Article]. *Paleontological Research*, 14(3), 179-195.
710 <https://doi.org/10.2517/1342-8144-14.3.179>
- 711 Sato, T., Zhao, L. J., Wu, X. C., & Li, C. (2014a). *Diandongosaurus acutidentatus*
712 Shang, Wu & Li, 2011 (Diapsida: Sauropterygia) and the relationships of
713 Chinese eosauroptrygians. *Geological Magazine*, 151(01), 121-133.
714 <http://dx.doi.org/10.1017/S0016756813000356>

- 715 Sato, T., Zhao, L. J., Wu, X. C., & Li, C. (2014b). A new specimen of the Triassic
716 pistosauroid *Yunguisaurus*, with implications for the origin of Plesiosauria
717 (Reptilia, Sauropterygia). *Palaeontology*, 57(1), 55-76.
718 <https://doi.org/10.1111/pala.12048>
- 719 Shang, Q. H., Sato, T., Li, C., & Wu, X. C. (2016). New osteological information
720 from a 'juvenile' specimen of *Yunguisaurus* (Sauropterygia; Pistosauroidea).
721 *Palaeoworld*, 26(3), 500-509.
722 <https://doi.org/http://dx.doi.org/10.1016/j.palwor.2016.05.008>
- 723 Shang, Q. H., Wu, X. C., & Li, C. (2020). A New Ladinian Nothosauroid
724 (Sauropterygia) from Fuyuan, Yunnan Province, China. *Journal of Vertebrate*
725 *Paleontology*, e1789651. <https://doi.org/10.1080/02724634.2020.1789651>
- 726 Shang, Q. H., & Li, C. (2015). A new small-sized eosauroptrygian (Diapsida:
727 Sauropterygia) from the Middle Triassic of Luoping, Yunnan, southwestern
728 China. *VERTEBRATA PALASIATICA*, 53(4), 265-280.
- 729 Shang, Q. H., Li, C., & Wu, X. C. (2017). New information on *Dianmeisaurus*
730 *gracilis* Shang & Li, 2015. *VERTEBRATA PALASIATICA*, 55(2), 145-161.
- 731 Shang, Q. H., Wu, X. C., & Li, C. (2011). A new eosauroptrygian from Middle
732 Triassic of eastern Yunnan Province, southwestern China. *VERTEBRATA*
733 *PALASIATICA*, 49(2), 155-171.

- 734 Storrs, G. W. (1991). Anatomy and relationships of *Corosaurus alcovensis* (Diapsida:
735 Sauropterygia) and the Triassic Alcova Limestone of Wyoming. *Bulletin of the*
736 *Peabody Museum of Natural History*, 44, 1-151.
- 737 Stubbs, T. L., & Benton, M. J. (2016). Ecomorphological diversifications of Mesozoic
738 marine reptiles: the roles of ecological opportunity and extinction. *Paleobiology*,
739 42(4), 547-573. <https://doi.org/doi:10.1017/pab.2016.15>
- 740 Sues, H. D., & Carroll, R. L. (1985). The pachypleurosaurid *Dactylosaurus*
741 *schroederi* (Diapsida: Sauropterygia). *Canadian Journal of Earth Sciences*,
742 22(11), 1602-1608.
- 743 Swofford, D. (2021). PAUP: phylogenetic analysis using parsimony (and other
744 methods), version 4.0. 1998. *Sinauer Sunderland, MA*.
- 745 Wang, X., Lu, H., Jiang, D. Y., Zhou, M., & Sun, Z.-Y. (2019). A new specimen of
746 *Yunguisaurus* (Reptilia; Sauropterygia) from the Ladinian (Middle Triassic)
747 Zhuganpo Member, Falang Formation, Guizhou, China and the restudy of
748 *Dingxiaosaurus*. *Palaeoworld*.
749 <https://doi.org/https://doi.org/10.1016/j.palwor.2019.05.006>
- 750 Wise, P. A., Vickaryous, M. K., & Russell, A. P. (2009). An embryonic staging table
751 for in ovo development of *Eublepharis macularius*, the leopard gecko. *The*
752 *Anatomical Record*, 292(8), 1198-1212.
- 753 Wu, X. C., Cheng, Y. N., Li, C., Zhao, L. J., & Sato, T. (2011). New information on
754 *Wumengosaurus delicatomandibularis* Jiang et al., 2008 (Diapsida:

755 Sauropterygia), with a revision of the osteology and phylogeny of the taxon.
 756 *Journal of Vertebrate Paleontology*, 31(1), 70-83.
 757 <http://www.informaworld.com/10.1080/02724634.2011.546724>
 758 Xu, G. H., Ren, Y., Zhao, L. J., Liao, J. L., & Feng, D. H. (2022). A long-tailed
 759 marine reptile from China provides new insights into the Middle Triassic
 760 pachypleurosaur radiation. *Sci Rep*, 12(1), 7396. [https://doi.org/10.1038/s41598-](https://doi.org/10.1038/s41598-022-11309-2)
 761 022-11309-2
 762 Xu, G. H., Shang, Q. H., Wang, W., Ren, Y., Lei, H., Liao, J. L., Zhao, L. J. & Li, C.
 763 (2023). A new long-snouted marine reptile from the Middle Triassic of China
 764 illuminates pachypleurosauroid evolution. *Sci Rep*, 13(1), 16.
 765 <https://doi.org/10.1038/s41598-022-24930-y>
 766 Zhao, L. J., Sato, T., & Li, C. (2008). The most complete pistosauroid skeleton from
 767 the Triassic of Yunnan, China. *Acta Geologica Sinica-English Edition*, 82(2),
 768 283-286.
 769
 770

Figure 1

[Click here to access/download;Figure;fig.1.tif](#)

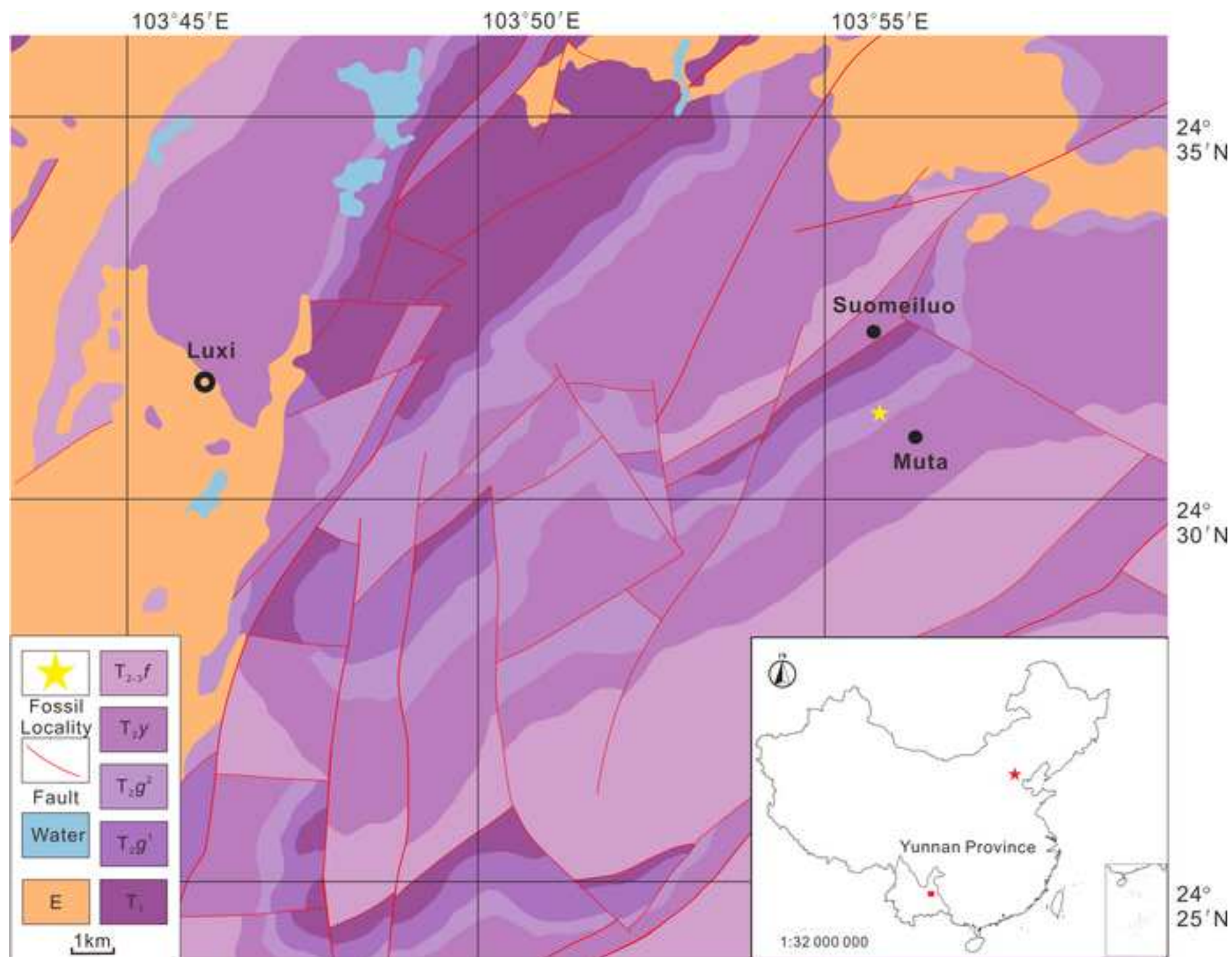


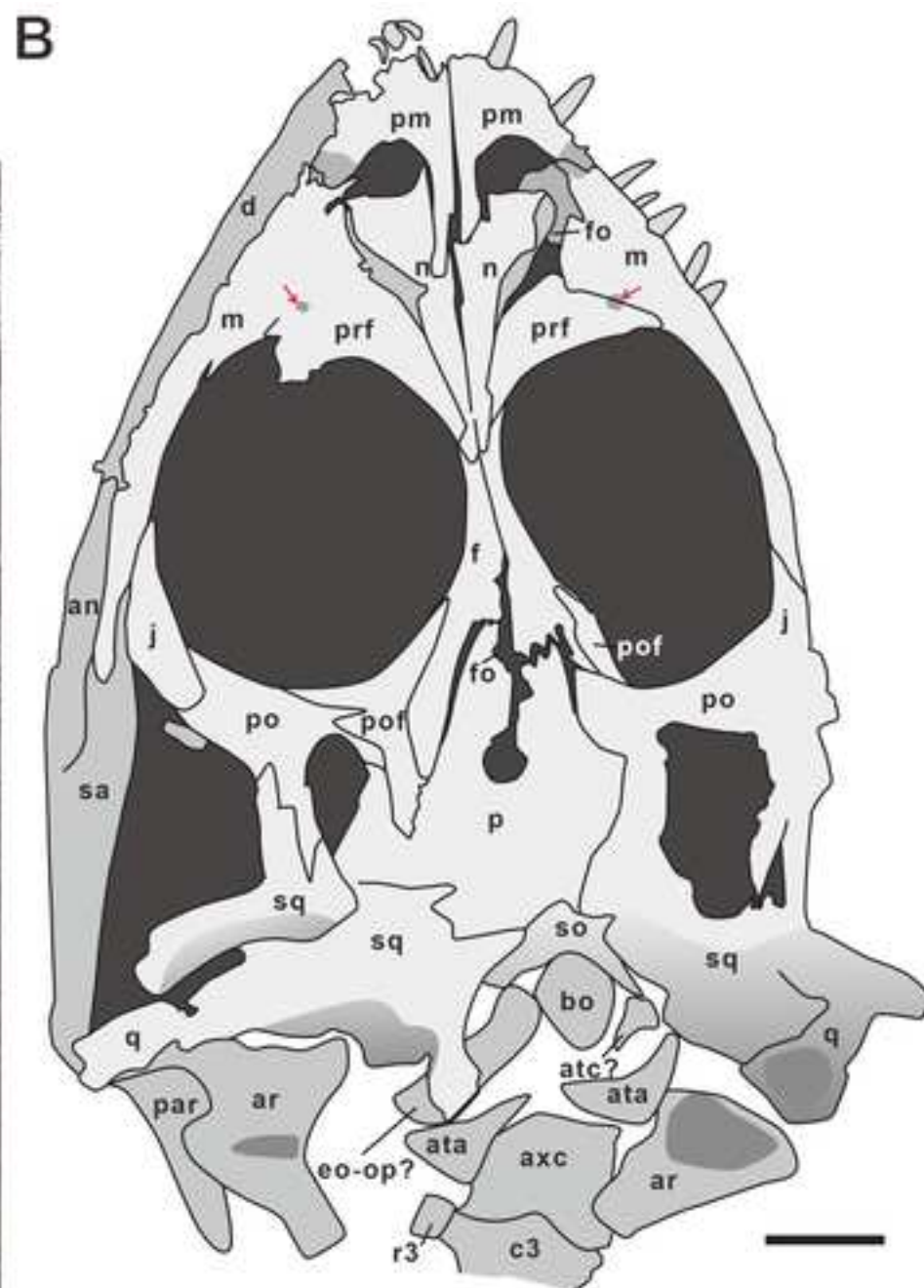
Figure 2

[Click here to access/download;Figure;fig.2.tif](#)



Figure 3

[Click here to access/download;Figure;fig.3 skull.tif](#)



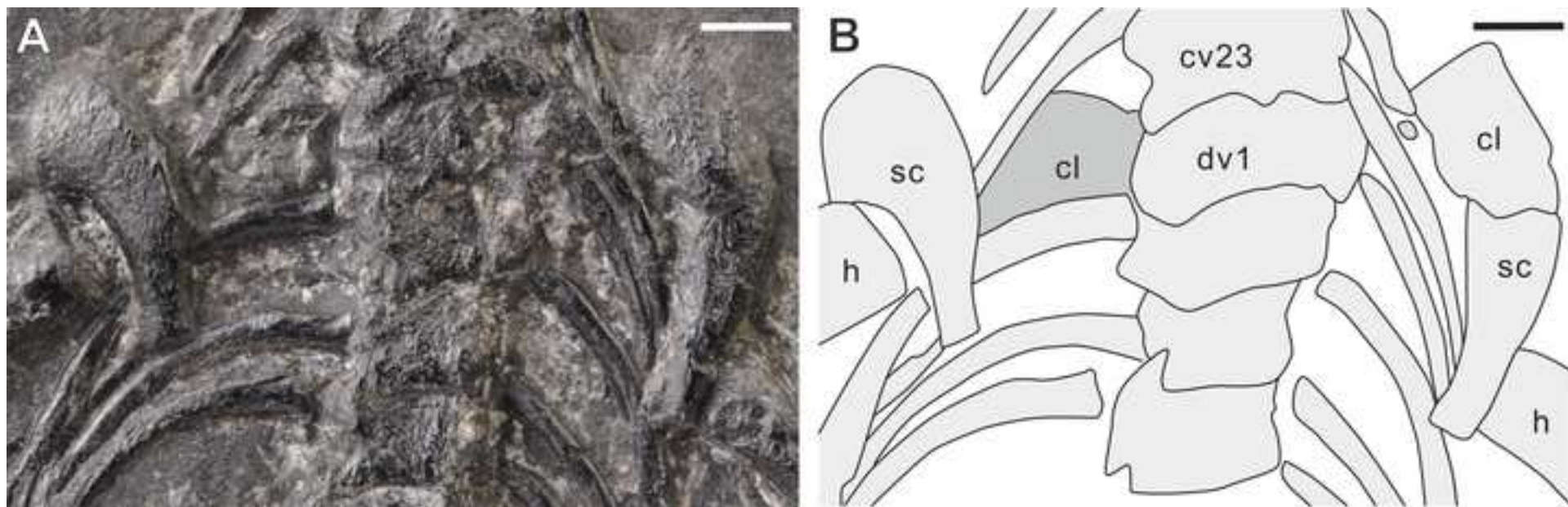
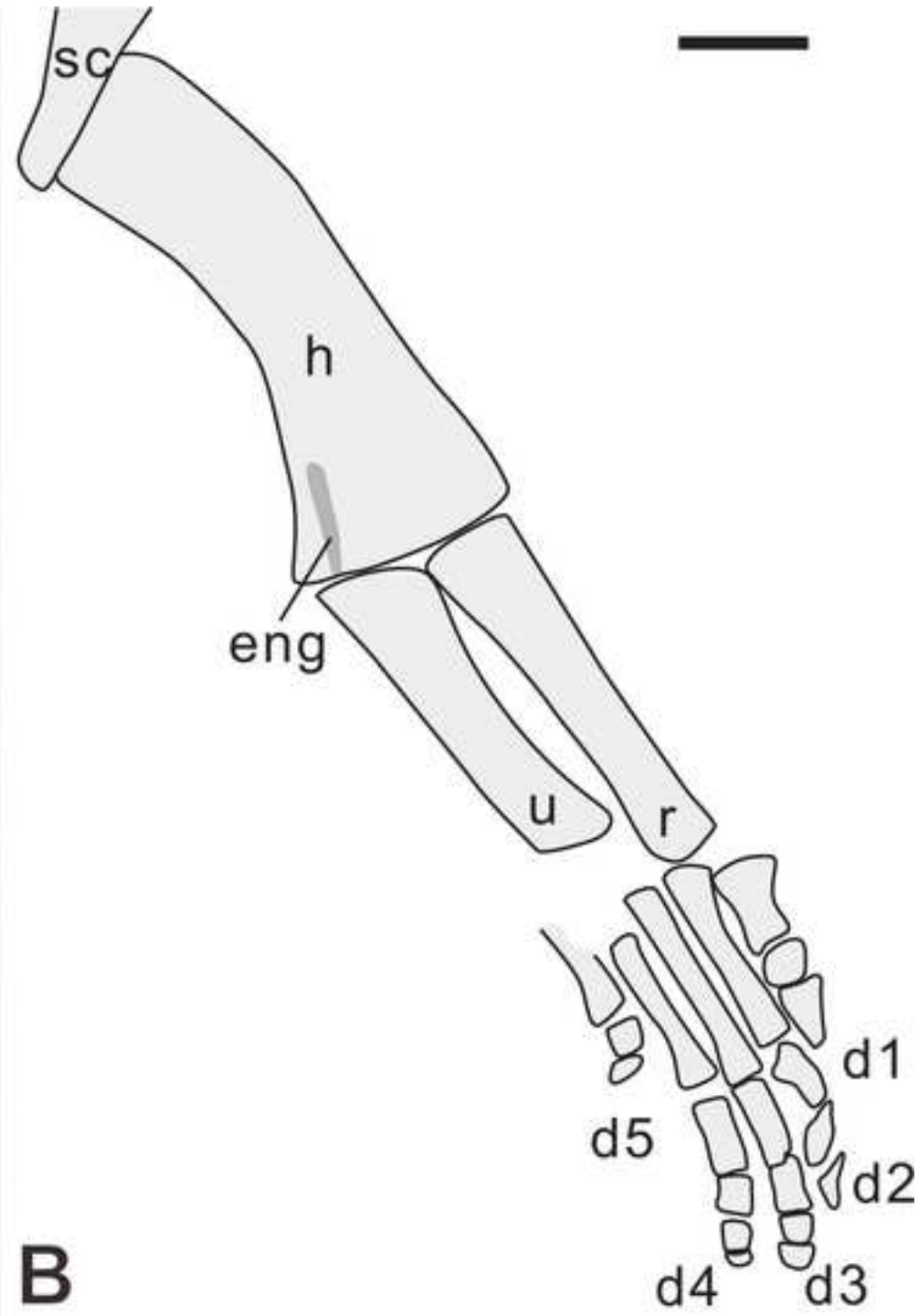


Figure 5



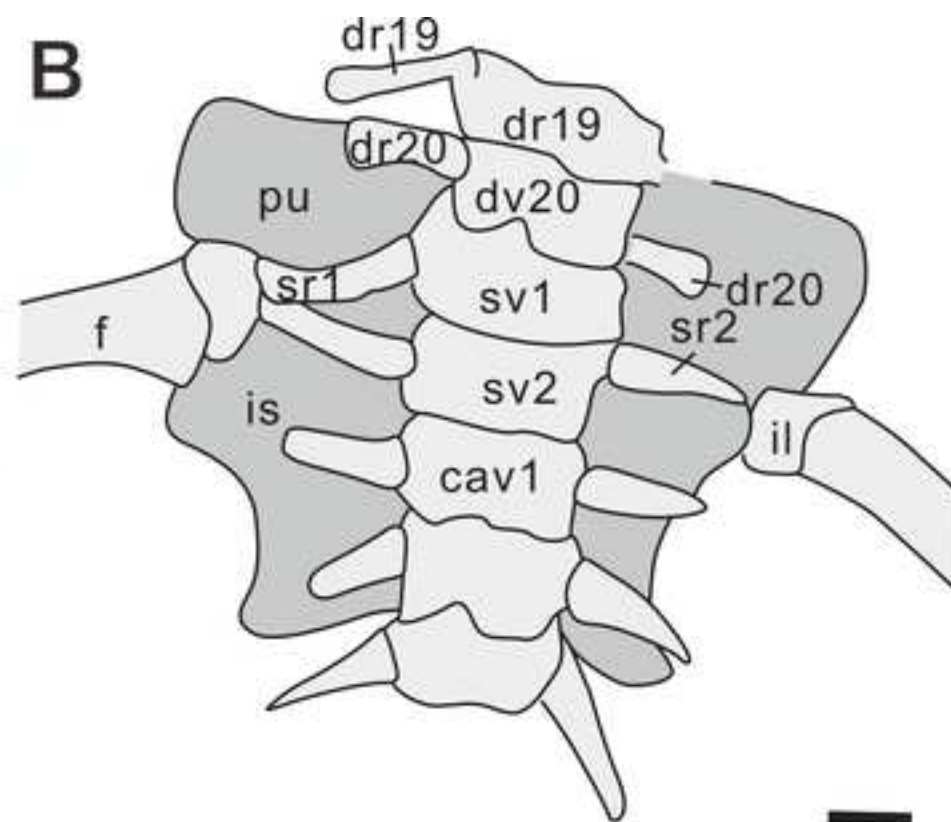


Figure 7

[Click here to access/download;Figure;fig.7.tif](#)

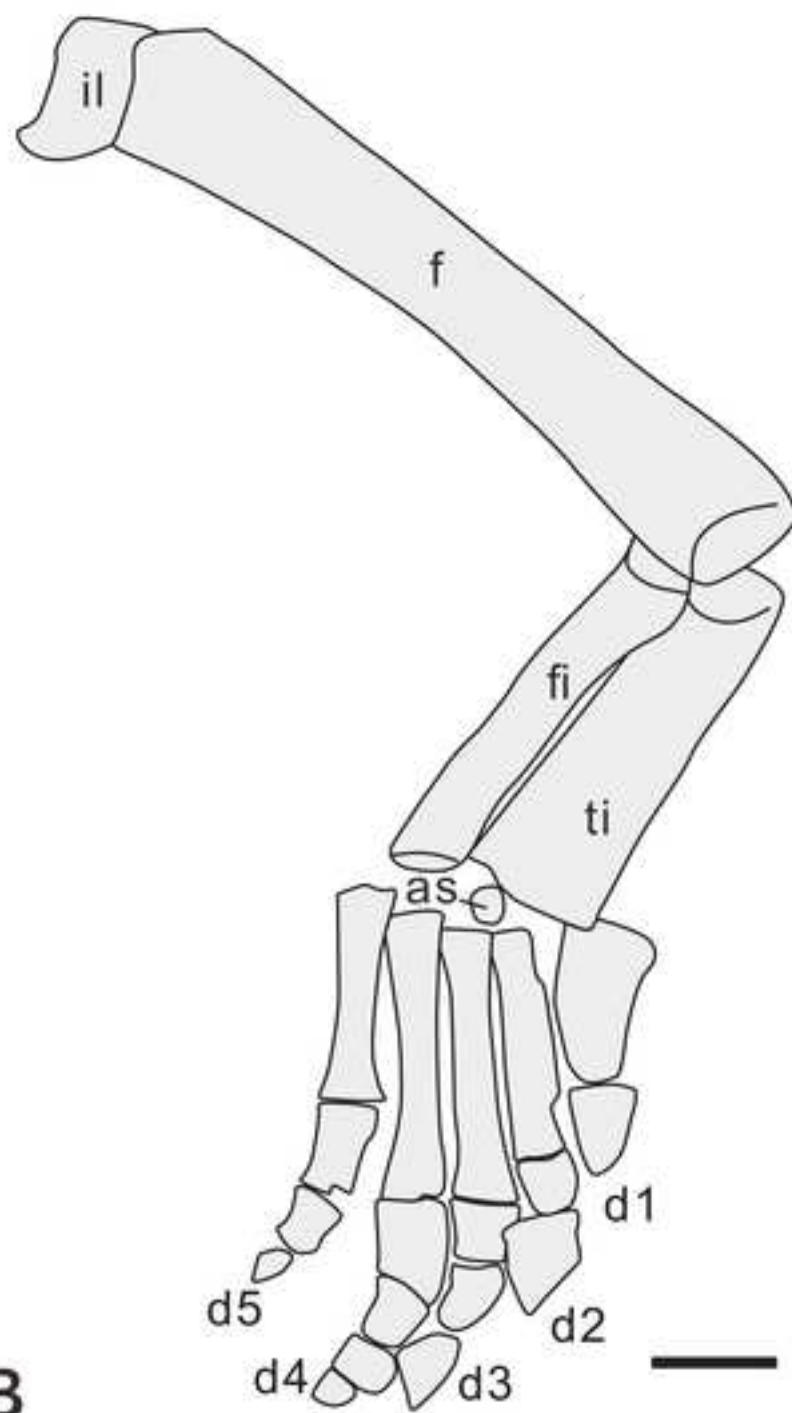
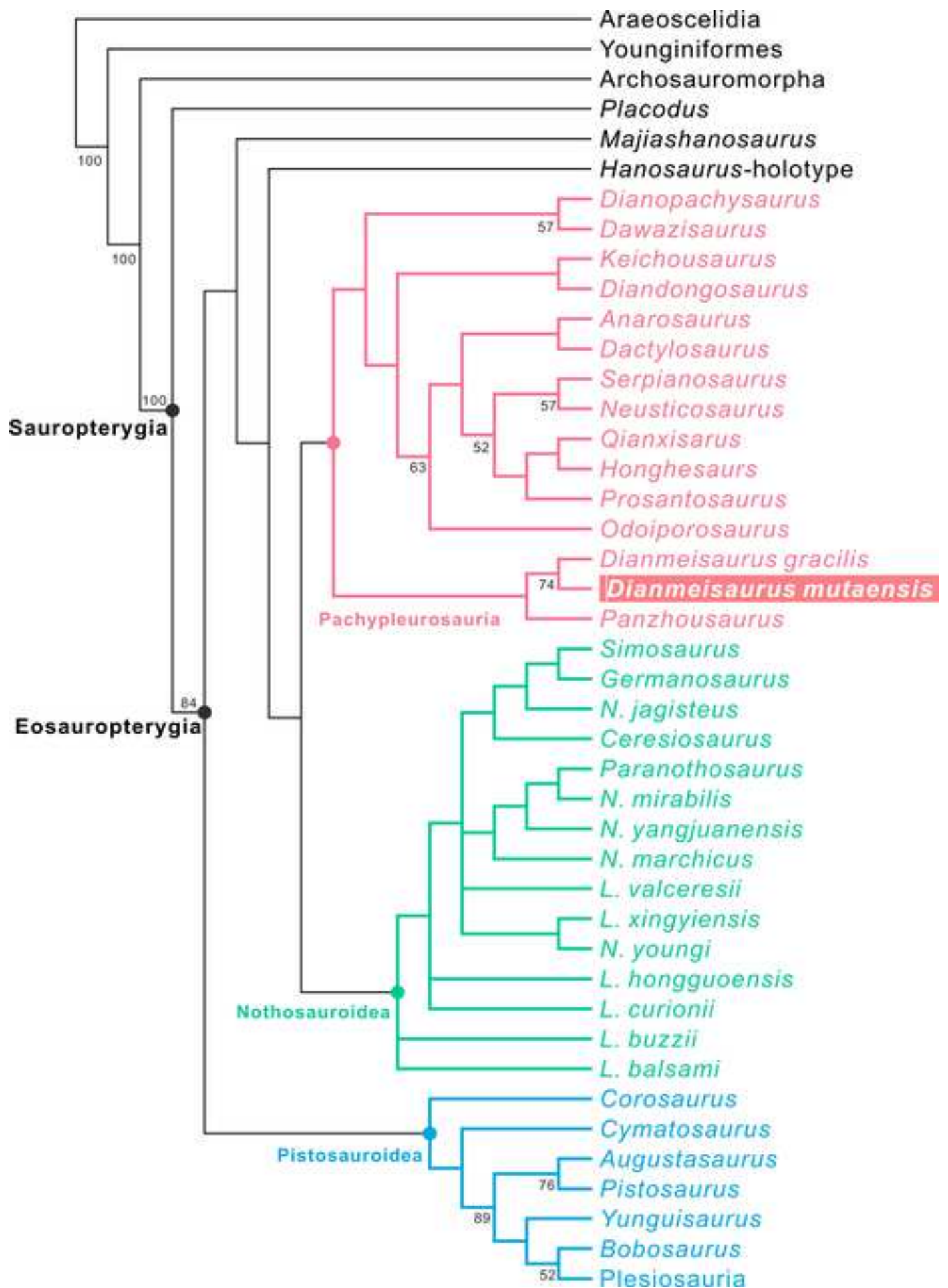
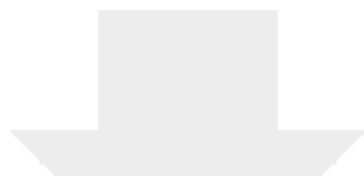


Figure 8





Click here to access/download
Supplementary Material
Supplemental Data 1.docx

